



Cite this: *Environ. Sci.: Adv.*, 2024, **3**, 28

Chitosan/PVA-supported silver nanoparticles for azo dyes removal: fabrication, characterization, and assessment of antioxidant activity†

Ismet Meydan,^{*a} Aysenur Aygun,^b Rima Nour Elhouda Tiri,^b Tugba Gur,^a Yilmaz Kocak,^c Hamdullah Seckin^a and Fatih Sen  ^{*a}

With the advancement of technology, studies in the field of nanotechnology have attracted great interest in recent years. The fact that nanomaterials have superior advantages over micromaterials provides a wide range of uses. Green synthesis is an effective way to prepare nanomaterials with an easy, fast, and environmentally friendly method. Within the scope of the study, AgNPs were synthesized using basil extract and combined with chitosan/PVA as a support material. By using chitosan/PVA support materials, the surface area of AgNPs was increased and it was aimed to improve their properties. The synthesized AgNPs@chitosan/PVA nanocomposite was characterized using various methods. In the UV-Vis spectrum, an absorbance peak was observed at 430 nm for the AgNPs@chitosan/PVA nanocomposite, and the particle size was determined as 25.10 nm according to TEM results. In addition, the photocatalytic and antioxidant activities of AgNPs@chitosan/PVA nanocomposite were investigated. The antioxidant activity of the AgNPs@chitosan/PVA (100 $\mu\text{g mL}^{-1}$) nanocomposite against DPPH and H_2O_2 was determined as 89.18% and 71.87%, respectively. The photocatalytic activity of the AgNPs@chitosan/PVA nanocomposite against methylene blue (MB), methylene red (MR), methylene orange (MO), safranin, and crystal violet (CV) dyes was 77%, 85%, 79%, 54%, and 9%, respectively. While the highest photocatalytic activity was observed against MR dye, very low photocatalytic activity was observed for CV. In light of the results obtained, it can be said that the AgNPs@chitosan/PVA nanocomposite has the potential to be used as an antioxidant agent and photocatalyst.

Received 7th August 2023
Accepted 25th October 2023

DOI: 10.1039/d3va00224a

rsc.li/esadvances

Environmental significance

Organic waste from the textile and other industrial dye-using activities has been causing more environmental problems for human society. These issues have been addressed using traditional chemical, biological, and physical wastewater treatment techniques, such as flotation, adsorption, chemical oxidation, solvent extraction, and filtration. However, some of these methods are expensive and some are not effective enough. Therefore, the use of photocatalysts for the cleaning of waste paints is one of the popular research topics of recent years. Within the scope of this study, AgNPs@chitosan/PVA was synthesized using *Ocimum basilicum* (basil) extract, and their photocatalytic and antioxidant activities was investigated. In addition, the photocatalytic activity of AgNPs@chitosan/PVA nanocomposite was determined by calculating the % photodegradation at the end of 90 minutes against MB, MR, MO, safranin, and CV dyes. The antioxidant activity of AgNPs@chitosan/PVA was determined against DPPH and H_2O_2 molecules.

1. Introduction

Nanomaterials can address a variety of technological and environmental issues in the fields of wastewater treatment, medicine, and solar energy conversion.^{1–3} Due to their wide

range of applications across numerous fields, researchers are now paying considerable attention to nanomaterials.^{4,5} The development of nanoscience and nanotechnology, which are concerned with the study of the properties of materials on the nanoscale and their wide range of applications in various fields, such as chemistry, biology, physics, and materials science, was made possible by Richard Feynman's 1959 lecture "There is Plenty of Room at the Bottom" and the invention of the scanning tunneling microscope in 1981. Owing to their high conductivity, high surface-to-volume ratio, plasmonic capabilities, and other characteristics, metal nanoparticles (MNPs) have long attracted much attention.^{6,7} A lot of research has been performed on modulating the surface plasmon

^aVan Vocational School of Health Services, Van Yuzuncu Yıl University, Zeve Campus, 65080, Van, Turkiye. E-mail: ismetmeydan@yyu.edu.tr; fatihsen1980@gmail.com

^bDepartment of Biochemistry, Sen Research Group, Dumlupınar University, 43000, Kütahya, Turkey

^cPhysical Therapy and Rehabilitation, Faculty of Health Sciences, Van Yuzuncu Yıl University, 65080, Van, Turkey

† Electronic supplementary information (ESI) available. See DOI: <https://doi.org/10.1039/d3va00224a>



resonance (SPR) of MNPs in order to determine how it might be used in sensors, biodevices, data storage, spectroscopic methods, catalysis, and other applications.⁸ SPR, which occurs when conduction electrons resonantly oscillate about the positive ion core under the right lighting conditions, is primarily influenced by the size, shape, and dielectric properties of the MNPs.⁹ To increase the sensitivity and resolution of optical systems, SPR capabilities can be used to amplify and manipulate light at the nanoscale.⁹ AgNPs are suited for several applications in a variety of fields, including catalysis, photonic, antibacterial, biosensing, and SERS substrates, due to their size-dependent characteristics.^{10,11} In order to increase biocompatibility, recent studies have looked into the adsorption of proteins on nanoparticles. This vast application potential has prompted a thorough search for growth techniques that can generate NPs of all forms and sizes.

Rapid urbanization, industrialization, and population growth are degrading the earth's atmosphere and releasing a vast quantity of dangerous and undesired compounds. Organic waste from textiles as well as other industrial dye-using activities have been causing more environmental problems for human society.¹² These issues have been addressed using traditional chemical, biological, and physical wastewater treatment techniques such as flotation, adsorption, chemical oxidation, solvent extraction, and filtration.¹³ Today, the use of nanomaterials for paint removal for cleaning wastewater has gained great importance.

AgNPs' adsorption capacity was raised by adding chitosan/PVA, and at the same time, photocatalytic performance was raised by encouraging the separation of electron-hole pairs. AgNPs show significant antioxidant, antibacterial, and anti-cancer properties.¹⁴ Due to its favored characteristics such as an antioxidant, antibacterial agent, superior biocompatibility, and biodegradability, chitosan has been used in domains such as tissue engineering and water treatment. It is used with PVA, to make up for some drawbacks such as low surface area, high cost, poor thermal and mechanical qualities, and dissolving in extremely acidic solutions.¹⁵

It is required to uncover the mysteries of natural products in order to develop the techniques used by nature to create NPs. Additionally, because NPs are frequently used in regions where people come in contact with them, there is an increasing need to create synthesis methods that do not include harmful substances. Due to the problems with the consumption of large amounts of energy, the release of toxic and harmful chemicals, and the use of complicated equipment and synthesis conditions, green synthesis methods are gradually replacing physical and chemical methods.¹⁶ As a result, the green/biological synthesis of NPs presents a potential substitute for chemical and physical processes. Therefore, more and more studies are focusing on environmentally friendly production of metals at the nanoscale.

Green nanoparticle synthesis is superior to previous approaches because it is straightforward, affordable, and mostly repeatable, and it frequently produces more stable compounds. The greatest choices appear to be materials made of herbs. They are ecologically friendly substitutes for

physical techniques and chemicals that are produced on a massive scale.¹⁷ Techniques using plants (leaves, roots, latex, seeds, and stems) and microbes might be used to synthesize naturally occurring metal nanoparticles. The key benefits of employing plants to create nanoparticles are availability, safe handling, and a high capacity for metabolite transformation when they can help with the reduction. The process of creating NPs from plants is not difficult; using plant extract, a metal salt is reduced, and the reaction is completed in a few minutes to a few hours. Extracts of natural products, enzymes, or proteins are used to reduce and stabilize NP formation.¹⁸ Reduction/oxidation is the primary process in the bottom-up method known as green nanoparticle production. The reduction of metal compounds into their own nanoparticles is mainly carried out by microbial enzymes or antioxidant phytochemicals found in plants.¹⁶ Given their potential to lessen NP toxicity, green synthesis techniques are quite appealing. As a result, using vitamins, amino acids, and plant extracts is becoming increasingly common.¹⁷

Phenolic compounds are the main active ingredients in some of these syntheses. The usage of non-toxic and ecologically friendly precursors is becoming more and more popular today. The primary concerns that require special consideration in a "green synthesis" method are the environment, the reduction of the reaction temperature, no releases of undesired by-products, and pollution.¹⁶

Within the scope of this study, AgNPs@chitosan/PVA was synthesized using the *Ocimum basilicum* (basil) extract, and their photocatalytic and antioxidant activities were investigated. The photocatalytic activity of AgNPs@chitosan/PVA nanocomposite was determined by calculating the % photo-degradation at the end of 90 minutes against MB, MR, MO, safranin, and CV dyes. AgNPs@chitosan/PVA antioxidant activity was determined against DPPH and H₂O₂ molecules.

2. Experiment

2.1. Extract of *Ocimum basilicum*

Dried *Ocimum basilicum* leaves were used in the preparation of the extract. The leaves were washed with distilled water (DW) until the impurities were removed and filtered. Then, 10 g of dry leaves were weighed and added into an Erlenmeyer flask containing 100 mL of DW and kept at 60 °C for 30 min. The resulting extract was filtered and kept at 4 °C.

2.2. Preparation of Ag NPs

To prepare Ag NPs, a 100 mL conical flask was used to combine 25 mL of produced aqueous basil leaf extract with 25 mL of AgNO₃ (0.5 M) solution. The solution was kept in a magnetic stirrer for 24 h, it was centrifuged 5 times and washed with DW and ethanol, and 48 hours of drying at 100 °C.

2.3. AgNPs@chitosan/PVA nanocomposite

The solution of 1% acetic acid was prepared, then 0.5 g of chitosan was dissolved in it at 70 °C with vigorous stirring until it



was completely soluble. 50 mL of DW was added to 0.5 g of PVA powder and stirred at 70 °C until a homogeneous solution was obtained. The chitosan solution (50/50% by weight) was added to the PVA solution under vigorous stirring to obtain a homogeneous chitosan/PVA solution. Then, AgNPs were added to the PVA/chitosan solution under sonication and mixed for 30 minutes.

2.4. Photodegradation of azo dyes

The photocatalytic property of AgNPs@chitosan/PVA nanocomposite was determined against methylene blue, methylene orange, methylene red, crystal violet, and safranin dyes in the presence of AgNPs@chitosan/PVA under sunlight.¹⁹ 10 mg of AgNPs@chitosan/PVA was added to DW and sonicated for 2 hours, then, 1 mg of dye powder was added to the solution and magnetically stirred for an additional 30 minutes in the dark. After 30 min, the colloidal suspension was exposed to sunlight. 5 mL of the colloidal suspension was taken every 30 min and scanned spectrophotometrically at 200 to 800 nm to examine the dye degradation.²⁰ The following equation was used to calculate the dye degradation (%).

$$\text{Photocatalytic degradation (\%)} = (C_0 - C_t)/C_0 \times 100 \quad (1)$$

C_0 = initial MB concentration and C_t = MB concentration after photoirradiation.

3. Results and discussion

3.1. Characterization

The UV-Vis spectrum of chitosan/PVA stabilized AgNPs is shown in Fig. 1a. The revealed surface plasmon resonance peaks were observed between 400–500 nm, typical for AgNPs.²¹ Surface plasmon resonances are highly dependent on the size, shape, and functionalization of metallic NPs.²² In Fig. 1b, the direct optical band gap energy E_g for AgNPs was calculated and found to be 2.30 eV. Shah *et al.* reported the optical band gap energy of AgNPs synthesized using *Plantago lanceolata* extract as 2.34 eV.²³ Fig. 1c shows the FTIR spectrum for AgNPs@chitosan/PVA. The band gap at 3290 cm^{-1} is associated with O-H and N-H stretching, and the bands at 2915 and 2850 cm^{-1} are associated with C-H and CH_2 ,^{24,25} respectively. The peaks at 1710, 1631, and 1420 cm^{-1} in the FTIR spectrum are attributed to carbonyl group stretching in the chitosan/PVA polymeric chains, NHCOCH_3 groups, and absorption of C-H bonds, respectively.²⁶ The peaks at 1375, 1244, 1081, 835, and 601 cm^{-1} may correspond to $-\text{CH}_3$ symmetrical deformation, C-N stretch band, C-O-C glycosidic ring, and metal-oxygen bond, respectively.^{19,20,27–30} Small peaks at 473 cm^{-1} can be attributed to its heterocyclic compounds, including alkaloids, and flavonoids from basil extract.²⁵ Fig. 1d shows the XRD pattern of AgNPs@chitosan/PVA nanocomposite. The peak at $2\theta = 21.98^\circ$ represents the chitosan@PVA complex. The peaks seen at $2\theta =$

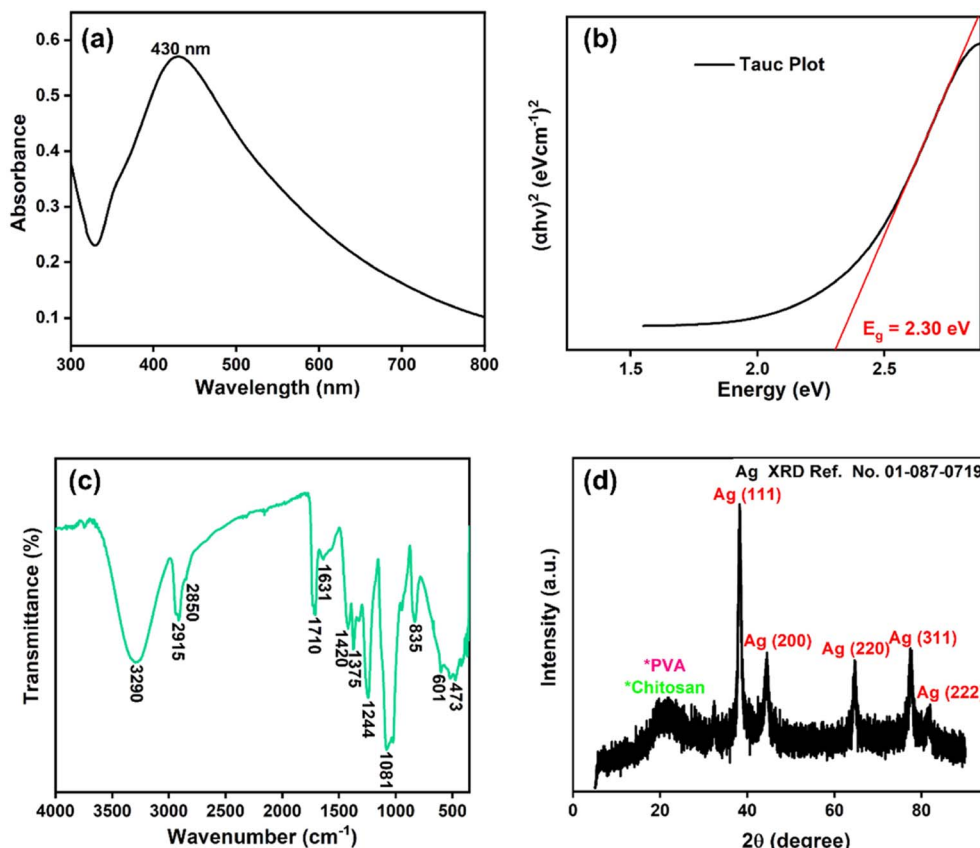


Fig. 1 (a) AgNPs@chitosan/PVA nanocomposite's Uv-vis spectra, (b) Tauc plot (c) FTIR spectrum, and (d) XRD pattern.



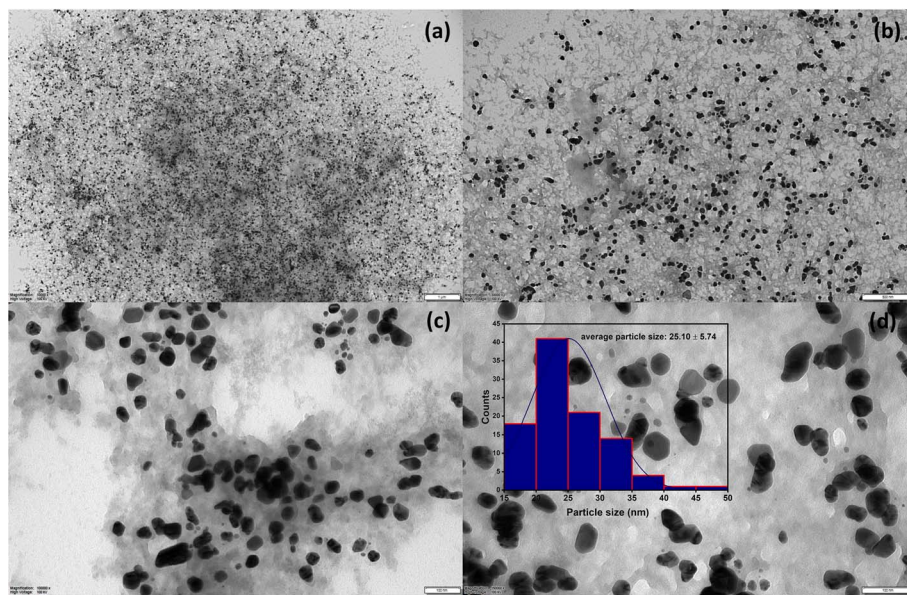


Fig. 2 TEM images at different scales (a; 1 μ m, b; 500 nm, (c and d); 100 nm) of AgNPs@chitosan/PVA nanocomposite and average particle size histogram.

38.24°, 44.52°, 64.65°, 77.42°, and 81.94° correspond to the Ag(111), Ag(200), Ag(220), Ag(311), and Ag(222) planes, respectively.^{21,31,32} The TEM image of AgNPs@chitosan/PVA nanocomposite is shown in Fig. 2. The morphological structure of the synthesized nanocomposite is spherical and monodisperse; the support material of chitosan/PVA can be seen quite clearly. The particle size histogram of AgNPs@chitosan/PVA is illustrated in Fig. 2 and the average particle size was found to be 25.10 ± 5.74 nm.

3.2. Antioxidant study against DPPH and H_2O_2

The antioxidant activity of AgNPs@chitosan/PVA nanocomposite was studied against DPPH and H_2O_2 . An increase in

DPPH radical scavenging activity was observed as the concentration of AgNPs@chitosan/PVA increased (Fig. 3). The best antioxidant activity was determined as 89.18% at 100 $\mu\text{g mL}^{-1}$ concentration. Ascorbic acid was used as a positive control for the determination of DPPH capture activity and the antioxidant activity was determined as 94.75%. It was determined that Ag@chitosan/PVA nanocomposite against H_2O_2 had peroxide clearance standards of 71.87% at 100 $\mu\text{g mL}^{-1}$, while ascorbic acid as a positive control had a peroxide clearance rate of 92.10% (Fig. 4). These results confirmed that AgNPs@chitosan/PVA had high antioxidant activity against DPPH and H_2O_2 . AgNPs@chitosan/PVA has high antioxidant activity against DPPH and H_2O_2 , but standard vitamin C (ascorbic acid) has

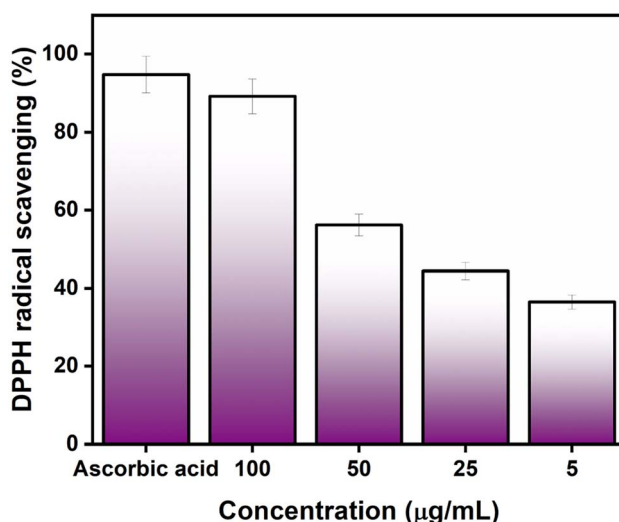


Fig. 3 Antioxidant activity of the Ag@Kitosan/PVA nanocomposite against the DPPH radical.

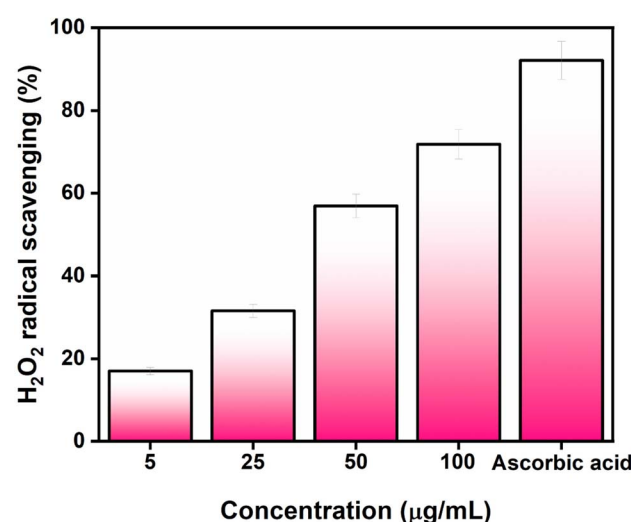


Fig. 4 Antioxidant activity of the Ag@Kitosan/PVA nanocomposite against H_2O_2 .



higher antioxidant activity.^{14,29,33} The antioxidant activity of chitosan–silver NPs, synthesized by the chemical reduction method with chitosan as a reducing agent, against DPPH was calculated as 60% for 10 mg mL⁻¹.³⁴ The antioxidant activity of Ag NPs produced from *Basella alba* leaf extract against DPPH and H₂O₂ was found to be 81.90% and 54.97%, respectively, at a concentration of 250 µg mL⁻¹.³⁵ The antioxidant activity of Ag NPs synthesized using *Bambusa arundinacea* extract against DPPH was found to be 61.5% and 74.4% for 100 and 200 µg mL⁻¹ concentrations, respectively.³⁶ Antioxidant activity of chitosan/PVA/ZnO nanofibrous membranes against DPPH was found to be in the range of 15.8–77% for the concentration range of 12.5–200 µg mL⁻¹.³⁷ The antioxidant activity of Ag NPs synthesized using *F. nygamai* isolate AJTYC1 against H₂O₂ at a concentration of 200 µg mL⁻¹ was determined to be 70.3%.³⁸

3.3. Photocatalytic activity of AgNPs@chitosan/PVA nanocomposite

The photocatalytic activity of the Ag@Kitosan/PVA nanocomposite was determined against MB, MR, MO, safranin, and CV dyes. Fig. 5a shows the photodegradation percentages of the dyes at different times, and the percentages of photodegradation rates for MB, MR, MO, safranin, and CV dyes at the end of 90 min were calculated as 77.41%, 85.44%, 81.69%, 54.50%, and 9.13%, respectively. Fig. 5b shows the C/C_0 (dye concentration) curves as a function of time, showing that the

Ag@Kitosan/PVA nanocomposite has an enhanced adsorption ability and photocatalytic performance for MB, MR, and MO dyes, and a high color change rate. At the end of the 90th minute, normal level photocatalytic activity was observed for safranin, but it was not possible to obtain photocatalytic activity for CV. Fig. 5c illustrates the kinetics of the Ag@Kitosan/PVA against the dyes that fit well with the first-order ratio equation. The rate constant (K' _{app}) was estimated using the first-order rate eqn (2).^{39,40} The reaction rate constant (k) and R^2 values for the photodegradation of the Ag@Kitosan/PVA nanocomposite are given in Table 1.

$$\ln(C_t/C_0) = -K'_\text{app} \cdot t \quad (2)$$

C_t and C_0 are the reactant concentrations at $t = t$ and $t = 0$, respectively.

Table 1 The reaction rate constant (k) and R^2 values against dyes used for photodegradation of Ag@Kitosan/PVA nanocomposite

Dye name	Rate constant	R^2 value
Methylene blue	0.0165	0.9521
Methylene red	0.0232	0.9389
Methylene orange	0.0181	0.9288
Safranine	0.008	0.8641
Crystal violet	0.001	0.9451

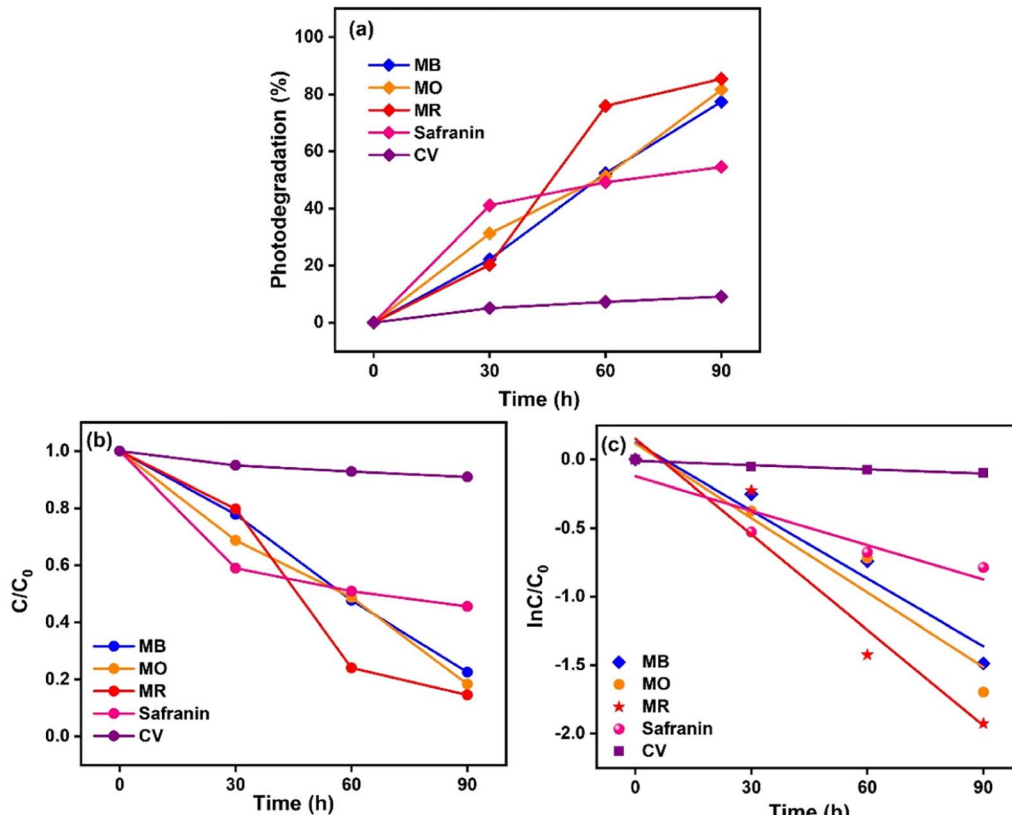


Fig. 5 (a) Degradation of dyes under sunlight (%), (b) degradation of dye solutions at versus time, (c) photodegradation kinetic study in the presence of Ag@Kitosan/PVA nanocomposite under sunlight.



Table 2 Comparison of the photocatalytic activity of the green synthesized Ag@Kitosan/PVA nanocomposite with various catalysts

Catalysts	Pollutants	Degradation (%)	Time (min)	References
PNHMA/Ag-AgCl-3	MO	78	270	43
D-AgNPs	MO	88	60	44
O-AgNPs		63		
S-AgNPs		62		
Biosynthesized ZnO NPs	MR	92.45	180	45
Mercury vanadate NPs	MB	50	90	46
	MR	75.5		
PdNi@VC NPs	Safranine	67	180	47
PbO NPs	CV	66.9	8 (h)	48
Co ₃ O ₄ NPs		63		
ZnO NPs		36		
Ag@Kitosan/PVA	MB	77.41	90	Present study
	MR	85.44	90	
	MO	81.69	90	
	Safranine	54.50	90	
	CV	9.13	90	

Silver-graphene (Ag-G) nanocomposite was synthesized by reducing Ag⁺ and graphene oxide using Mortiño fruit extract as the reducing agent, and its photocatalytic activity against MO dye was found to be 84% after 120 min.⁴¹ Silver-doped titanium dioxide nanoparticles were synthesized using *Nephelium lappaceum* L. bark extract, and the photodegradation rate against MB dye was reported to be 81% at the end of 600 min.⁴² Table 2 shows the photocatalytic activities of Ag@chitosan/PVA and the different catalysts.

4. Conclusion

The Ag@chitosan/PVA nanocomposite was synthesized using the green synthesis method and chitosan/PVA was used as the support material. The Ag@chitosan/PVA nanocomposite showed antioxidant and photocatalytic activity properties by providing a large surface area for AgNPs. The characterization, structural, morphological, and size of AgNPs@chitosan/PVA were determined by UV-Vis, FTIR, XRD, and TEM analyses. The synthesized AgNPs@chitosan/PVA nanocomposite was crystalline and exhibited a sharp SPR bandwidth at 430 nm. TEM analysis showed the formation of Ag NPs with an average size of 25.10 ± 5.74 nm and a homogeneous spread over the chitosan@PVA complex. The antioxidant properties of AgNPs@chitosan/PVA nanocomposite were determined and found to be 89.18% and 71.87% against DPPH and H₂O₂, respectively.

The synthesized AgNPs@chitosan/PVA nanocomposite could have potential applications as free radical scavengers in the treatment of various diseases. Therefore, it can be concluded that AgNPs@chitosan/PVA nanocomposite may be a gateway to the treatment of various health problems. The photocatalytic activity of the AgNPs@chitosan/PVA nanocomposite against MB, MR, MO, safranin, and CV dyes after 90 minutes was determined to be 77.41%, 85.44%, 81.69%, 54.50%, and 9.13%, respectively. These results show that AgNPs@chitosan/PVA can be developed as an excellent photocatalyst to treat wastewater pollution from textile dyes such as MB, MR, and MO.

Conflicts of interest

The authors declare that there is no conflict of interest regarding the publication of this article.

Acknowledgements

The authors would like to thank the Van Yuzuncu Yil University Scientific Projects Research Office (Project Number FBA-2022-9841) for funding. A. Aygun is supported by the Council of Higher Education (CoHE) with a 100/2000 PhD Scholarship.

References

- 1 R. Darabi, F. E. D. Alown, A. Aygun, Q. Gu, F. Gulbagca, E. E. Altuner, *et al.*, Biogenic platinum-based bimetallic nanoparticles: Synthesis, characterization, antimicrobial activity and hydrogen evolution, *Int. J. Hydrogen Energy*, 2023, **48**(55), 21270–21284, DOI: [10.1016/j.ijhydene.2022.12.072](https://doi.org/10.1016/j.ijhydene.2022.12.072).
- 2 R. Darabi and H. Karimi-Maleh, Hierarchical copper-1,3,5 benzenetricarboxylic acid-MOF-derived with nitrogen-doped graphene nanoribbons as a novel assembly nanocomposite for asymmetric supercapacitors, *Adv. Compos. Hybrid Mater.*, 2023, **6**, 1–10, DOI: [10.1007/S42114-023-00696-3](https://doi.org/10.1007/S42114-023-00696-3).
- 3 H. Lim, T. Nagaura, M. Kim, K. Kani, J. Kim, Y. Bando, *et al.*, Electrochemical preparation system for unique mesoporous hemisphere gold nanoparticles using block copolymer micelles, *RSC Adv.*, 2020, **10**, 8309–8313, DOI: [10.1039/d0ra01072c](https://doi.org/10.1039/d0ra01072c).
- 4 Y. Kocak, I. Meydan, T. Gur Karahan and F. Sen, Investigation of mycosynthesized silver nanoparticles by the mushroom *Pleurotus eryngii* in biomedical applications, *Int. J. Environ. Sci. Technol.*, 2023, 1–12, DOI: [10.1007/S13762-023-04786-z](https://doi.org/10.1007/S13762-023-04786-z).
- 5 H. Lim, D. Kim, Y. Kim, T. Nagaura, J. You, J. Kim, *et al.*, A mesopore-stimulated electromagnetic near-field:



electrochemical synthesis of mesoporous copper films by micelle self-assembly, *J. Mater. Chem. A*, 2020, **8**, 21016–21025, DOI: [10.1039/d0ta06228f](https://doi.org/10.1039/d0ta06228f).

6 S. Jain and M. S. Mehata, Medicinal Plant Leaf Extract and Pure Flavonoid Mediated Green Synthesis of Silver Nanoparticles and their Enhanced Antibacterial Property, *Sci. Rep.*, 2017, **7**(7), 1–13, DOI: [10.1038/s41598-017-15724-8](https://doi.org/10.1038/s41598-017-15724-8).

7 M. S. Mehata, M. Majumder, B. Mallik and N. Ohta, External electric field effects on optical property and excitation dynamics of capped CdS quantum dots embedded in a polymer film, *J. Phys. Chem. C*, 2010, **114**, 15594–15601, DOI: [10.1021/jp104124z](https://doi.org/10.1021/jp104124z).

8 K. Kamakshi, J. P. B. Silva, K. C. Sekhar, G. Marslin, J. A. Moreira, O. Conde, *et al.*, Influence of substrate temperature on the properties of pulsed laser deposited silver nanoparticle thin films and their application in SERS detection of bovine serum albumin, *Appl. Phys. B: Lasers Opt.*, 2016, **122**, 1–8, DOI: [10.1007/S00340-016-6385-0](https://doi.org/10.1007/S00340-016-6385-0).

9 M. A. Garcia, Surface plasmons in metallic nanoparticles: fundamentals and applications, *J. Phys. D Appl. Phys.*, 2011, **44**, 283001, DOI: [10.1088/0022-3727/44/28/283001](https://doi.org/10.1088/0022-3727/44/28/283001).

10 K. Kamakshi, K. C. Sekhar, A. Almeida, J. Agostinho Moreira and M. J. M. Gomes, Tuning the surface plasmon resonance and surface-enhanced Raman scattering of pulsed laser deposited silver nanoparticle films by ambience and deposition temperature, *J. Opt.*, 2014, **16**, 055002, DOI: [10.1088/2040-8978/16/5/055002](https://doi.org/10.1088/2040-8978/16/5/055002).

11 H. Lim, D. Kim, G. Kwon, H. J. Kim, J. You, J. Kim, *et al.*, Synthesis of Uniformly Sized Mesoporous Silver Films and Their SERS Application, *J. Phys. Chem. C*, 2020, **124**, 23730–23737, DOI: [10.1021/ACS.JPCC.0C07234](https://doi.org/10.1021/ACS.JPCC.0C07234).

12 Y. Zhou, S. Fang, M. Zhou, G. Wang, S. Xue, Z. Li, *et al.*, Fabrication of novel ZnFe₂O₄/BiOI nanocomposites and its efficient photocatalytic activity under visible-light irradiation, *J. Alloys Compd.*, 2017, **696**, 353–361, DOI: [10.1016/J.jallcom.2016.11.323](https://doi.org/10.1016/J.jallcom.2016.11.323).

13 L. L. Zhang, L. Zhan, Y. D. Jin, Z. L. Min, C. Wei, Q. Wang, *et al.*, SIRT2 mediated antitumor effects of shikonin on metastatic colorectal cancer, *Eur. J. Pharmacol.*, 2017, **797**, 1–8, DOI: [10.1016/J.ejphar.2017.01.008](https://doi.org/10.1016/J.ejphar.2017.01.008).

14 A. K. Keshari, R. Srivastava, P. Singh, V. B. Yadav and G. Nath, Antioxidant and antibacterial activity of silver nanoparticles synthesized by *Cestrum nocturnum*, *J. Ayurveda Integr. Med.*, 2020, **11**, 37–44, DOI: [10.1016/j.jaim.2017.11.003](https://doi.org/10.1016/j.jaim.2017.11.003).

15 W. Yang, E. Fortunati, F. Bertoglio, J. S. Owczarek, G. Bruni, M. Kozanecki, *et al.*, Polyvinyl alcohol/chitosan hydrogels with enhanced antioxidant and antibacterial properties induced by lignin nanoparticles, *Carbohydr. Polym.*, 2018, **181**, 275–284, DOI: [10.1016/J.carbpol.2017.10.084](https://doi.org/10.1016/J.carbpol.2017.10.084).

16 D. Horwat, D. I. Zakharov, J. L. Endrino, F. Soldera, A. Anders, S. Migot, *et al.*, Chemistry, phase formation, and catalytic activity of thin palladium-containing oxide films synthesized by plasma-assisted physical vapor deposition, *Surf. Coat. Technol.*, 2011, **205**, S171–S177, DOI: [10.1016/J.surfcoat.2010.12.021](https://doi.org/10.1016/J.surfcoat.2010.12.021).

17 M. Gholami-Shabani, M. Shams-Ghahfarokhi, Z. Gholami-Shabani, A. Akbarzadeh, G. Riazi, S. Ajdari, *et al.*, Enzymatic synthesis of gold nanoparticles using sulfite reductase purified from *Escherichia coli*: A green eco-friendly approach, *Process Biochem.*, 2015, **50**, 1076–1085, DOI: [10.1016/J.procbio.2015.04.004](https://doi.org/10.1016/J.procbio.2015.04.004).

18 B. Baruwati, V. Polshettiwar and R. S. Varma, Glutathione promoted expeditious green synthesis of silver nanoparticles in water using microwaves, *Green Chem.*, 2009, **11**, 926–930, DOI: [10.1039/b902184a](https://doi.org/10.1039/b902184a).

19 M. K. Sahu and R. K. Patel, Novel visible-light-driven cobalt loaded neutralized red mud (Co/NRM) composite with photocatalytic activity toward methylene blue dye degradation, *J. Ind. Eng. Chem.*, 2016, **40**, 72–82, DOI: [10.1016/j.jiec.2016.06.008](https://doi.org/10.1016/j.jiec.2016.06.008).

20 V. Ravichandran, S. Vasanthi, S. Shalini, S. A. A. Shah, M. Tripathy and N. Paliwal, Green synthesis, characterization, antibacterial, antioxidant and photocatalytic activity of *Parkia speciosa* leaves extract mediated silver nanoparticles, *Results Phys.*, 2019, **15**, 102565, DOI: [10.1016/j.rinp.2019.102565](https://doi.org/10.1016/j.rinp.2019.102565).

21 E. D. Cavassin, L. F. P. de Figueiredo, J. P. Otoch, M. M. Seckler, R. A. de Oliveira, F. F. Franco, *et al.*, Comparison of methods to detect the in vitro activity of silver nanoparticles (AgNP) against multidrug resistant bacteria, *J. Nanobiotechnol.*, 2015, **13**, 1–16, DOI: [10.1186/S12951-015-0120-6](https://doi.org/10.1186/S12951-015-0120-6).

22 E. A. Coronado, E. R. Encina and F. D. Stefani, Optical properties of metallic nanoparticles: manipulating light, heat and forces at the nanoscale, *Nanoscale*, 2011, **3**, 4042–4059, DOI: [10.1039/c1nr10788g](https://doi.org/10.1039/c1nr10788g).

23 M. Z. Shah, Z. H. Guan, A. U. Din, A. Ali, A. U. Rehman, K. Jan, *et al.*, Synthesis of silver nanoparticles using *Plantago lanceolata* extract and assessing their antibacterial and antioxidant activities, *Sci. Rep.*, 2021, **11**, 1–14, DOI: [10.1038/s41598-021-00296-5](https://doi.org/10.1038/s41598-021-00296-5).

24 Z. Nate, M. J. Moloto, P. K. Mubiayi and P. N. Sibiya, Green synthesis of chitosan capped silver nanoparticles and their antimicrobial activity, *MRS Adv.*, 2018, **342**(3), 2505–2517, DOI: [10.1557/adv.2018.368](https://doi.org/10.1557/adv.2018.368).

25 K. Kalantari, E. Mostafavi, B. Saleh, P. Soltantabar and T. J. Webster, Chitosan/PVA hydrogels incorporated with green synthesized cerium oxide nanoparticles for wound healing applications, *Eur. Polym. J.*, 2020, **134**, 109853, DOI: [10.1016/J.eurpolymj.2020.109853](https://doi.org/10.1016/J.eurpolymj.2020.109853).

26 S. Agnihotri, S. Mukherji and S. Mukherji, Antimicrobial chitosan–PVA hydrogel as a nanoreactor and immobilizing matrix for silver nanoparticles, *Appl. Nanosci.*, 2012, **23**(2), 179–188, DOI: [10.1007/S13204-012-0080-1](https://doi.org/10.1007/S13204-012-0080-1).

27 V. A. Pereira, I. N. Q. de Arruda and R. Stefani, Active chitosan/PVA films with anthocyanins from *Brassica oleracea* (Red Cabbage) as Time–Temperature Indicators for application in intelligent food packaging, *Food Hydrocolloids*, 2015, **43**, 180–188, DOI: [10.1016/J.foodhyd.2014.05.014](https://doi.org/10.1016/J.foodhyd.2014.05.014).

28 D. M. Suflet, I. Popescu, I. M. Pelin, D. L. Ichim, O. M. Daraba, M. Constantin, *et al.*, Dual Cross-Linked

Chitosan/PVA Hydrogels Containing Silver Nanoparticles with Antimicrobial Properties, *Pharm.*, 2021, **13**, 1461, DOI: [10.3390/pharmaceutics13091461](https://doi.org/10.3390/pharmaceutics13091461).

29 A. Sudha, J. Jeyakanthan and P. Srinivasan, Green synthesis of silver nanoparticles using *Lippia nodiflora* aerial extract and evaluation of their antioxidant, antibacterial and cytotoxic effects, *Resour. Technol.*, 2017, **3**, 506–515, DOI: [10.1016/J.refft.2017.07.002](https://doi.org/10.1016/J.refft.2017.07.002).

30 P. Rani, V. Kumar, P. P. Singh, A. S. Matharu, W. Zhang, K. H. Kim, *et al.*, Highly stable AgNPs prepared via a novel green approach for catalytic and photocatalytic removal of biological and non-biological pollutants, *Environ. Int.*, 2020, **143**, 105924, DOI: [10.1016/J.envint.2020.105924](https://doi.org/10.1016/J.envint.2020.105924).

31 H. M. Ibrahim, S. Zaghloul, M. Hashem and A. El-Shafei, A green approach to improve the antibacterial properties of cellulose based fabrics using *Moringa oleifera* extract in presence of silver nanoparticles, *Cellulose*, 2021, **28**, 549–564, DOI: [10.1007/S10570-020-03518-7](https://doi.org/10.1007/S10570-020-03518-7).

32 M. E. I. Badawy, T. M. R. Lotfy and S. M. S. Shawir, Preparation and antibacterial activity of chitosan-silver nanoparticles for application in preservation of minced meat, *Bull. Natl. Res. Cent.*, 2019, **431**, 1–14, DOI: [10.1186/S42269-019-0124-8](https://doi.org/10.1186/S42269-019-0124-8).

33 D. Bharathi and V. Bhuvaneshwari, Evaluation of the Cytotoxic and Antioxidant Activity of Phyto-synthesized Silver Nanoparticles Using *Cassia angustifolia* Flowers, *Bionanoscience*, 2019, **9**, 155–163, DOI: [10.1007/S12668-018-0577-5](https://doi.org/10.1007/S12668-018-0577-5).

34 P. K. Dara, R. Mahadevan, P. A. Digita, S. Visnuvinayagam, L. R. G. Kumar, S. Mathew, *et al.*, Synthesis and biochemical characterization of silver nanoparticles grafted chitosan (Chi-Ag-NPs): in vitro studies on antioxidant and antibacterial applications, *SN Appl. Sci.*, 2020, **24**(2), 1–12, DOI: [10.1007/S42452-020-2261-Y](https://doi.org/10.1007/S42452-020-2261-Y).

35 M. Mani, S. Pavithra, K. Mohanraj, S. Kumaresan, S. S. Alotaibi, M. M. Eraqi, *et al.*, Studies on the spectrometric analysis of metallic silver nanoparticles (Ag NPs) using *Basella alba* leaf for the antibacterial activities, *Environ. Res.*, 2021, **199**, 111274, DOI: [10.1016/J.envres.2021.111274](https://doi.org/10.1016/J.envres.2021.111274).

36 N. Jayarambabu, S. Velupla, A. Akshaykranth, N. Anitha and T. V. Rao, *Bambusa arundinacea* leaves extract-derived Ag NPs: evaluation of the photocatalytic, antioxidant, antibacterial, and anticancer activities, *Appl. Phys. A: Mater. Sci. Process.*, 2023, **129**, 1–10, DOI: [10.1007/S00339-022-06279-1](https://doi.org/10.1007/S00339-022-06279-1).

37 R. Ahmed, M. Tariq, I. Ali, R. Asghar, P. Noorunnisa Khanam, R. Augustine, *et al.*, Novel electrospun chitosan/polyvinyl alcohol/zinc oxide nanofibrous mats with antibacterial and antioxidant properties for diabetic wound healing, *Int. J. Biol. Macromol.*, 2018, **120**, 385–393, DOI: [10.1016/J.ijbiomac.2018.08.057](https://doi.org/10.1016/J.ijbiomac.2018.08.057).

38 A. E. El-Ansary, A. A. A. Omran, H. I. Mohamed and O. M. El-Mahdy, Green synthesized silver nanoparticles mediated by *Fusarium nygamai* isolate AJTYC1: characterizations, antioxidant, antimicrobial, anticancer, and photocatalytic activities and cytogenetic effects, *Environ. Sci. Pollut. Res.*, 2023, **1**, 1–23, DOI: [10.1007/S11356-023-29414-8](https://doi.org/10.1007/S11356-023-29414-8).

39 F. Karimi, R. N. Elhouda Tiri, A. Aygun, F. Gulbagca, S. Özdemir, S. Gonca, *et al.*, One-step synthesized biogenic nanoparticles using *Linum usitatissimum*: Application of sun-light photocatalytic, biological activity and electrochemical H_2O_2 sensor, *Environ. Res.*, 2023, **218**, 114757, DOI: [10.1016/j.envres.2022.114757](https://doi.org/10.1016/j.envres.2022.114757).

40 F. Ameen, A. Aygun, A. Seyrankaya, R. N. Elhouda Tiri, F. Gulbagca, İ. Kaynak, *et al.*, Photocatalytic investigation of textile dyes and *E. coli* bacteria from wastewater using $Fe_3O_4@MnO_2$ heterojunction and investigation for hydrogen generation on $NaBH_4$ hydrolysis, *Environ. Res.*, 2023, **220**, 115231, DOI: [10.1016/j.envres.2023.115231](https://doi.org/10.1016/j.envres.2023.115231).

41 K. S. Vizuete, B. Kumar, A. V. Vaca, A. Debut and L. Cumbal, Mortiño (*Vaccinium floribundum* Kunth) berry assisted green synthesis and photocatalytic performance of Silver-Graphene nanocomposite, *J. Photochem. Photobiol. A*, 2016, **329**, 273–279, DOI: [10.1016/J.jphotochem.2016.06.030](https://doi.org/10.1016/J.jphotochem.2016.06.030).

42 B. Kumar, K. Smita, Y. Angulo and L. Cumbal, Valorization of rambutan peel for the synthesis of silver-doped titanium dioxide (Ag/TiO_2) nanoparticles, *Green Process. Synth.*, 2016, **5**, 371–377, DOI: [10.1515/GPS-2016-0003/machinereadablecitation/RIS](https://doi.org/10.1515/GPS-2016-0003/machinereadablecitation/RIS).

43 Y. Zou, H. Huang, S. Li, J. Wang and Y. Zhang, Synthesis of supported $Ag/AgCl$ composite materials and their photocatalytic activity, *J. Photochem. Photobiol. A*, 2019, **376**, 43–53, DOI: [10.1016/J.jphotochem.2019.03.008](https://doi.org/10.1016/J.jphotochem.2019.03.008).

44 S. Hasan and A. Rauf, A comparative analysis of photocatalytic activity against methyl orange with C18 derivatives of fatty acid coated Ag/Ag_2O nanoparticles, *Mater. Today: Proc.*, 2021, **46**, 2975–2981, DOI: [10.1016/J.matpr.2020.12.500](https://doi.org/10.1016/J.matpr.2020.12.500).

45 L. Fu and Z. Fu, *Plectranthus amboinicus* leaf extract-assisted biosynthesis of ZnO nanoparticles and their photocatalytic activity, *Ceram. Int.*, 2015, **41**, 2492–2496, DOI: [10.1016/J.ceramint.2014.10.069](https://doi.org/10.1016/J.ceramint.2014.10.069).

46 S. B. Dhanalekshmi, R. Priya, K. Tamizh Selvi, K. Alamelu Mangai, G. K. Weldegebrieal, S. Garg, *et al.*, Microwave-assisted synthesis, characterization and photocatalytic activity of mercury vanadate nanoparticles, *Inorg. Chem. Commun.*, 2021, **131**, 108768, DOI: [10.1016/J.inoche.2021.108768](https://doi.org/10.1016/J.inoche.2021.108768).

47 F. Ameen, R. N. E. Tiri, M. Bekmezci, F. Karimi, N. Bennini and F. Sen, Microwave-assisted synthesis of Vulcan Carbon supported Palladium–Nickel ($PdNi@VC$) bimetallic nanoparticles, and investigation of antibacterial and Safranine dye removing effects, *Chemosphere*, 2023, **339**, 139630, DOI: [10.1016/J.chemosphere.2023.139630](https://doi.org/10.1016/J.chemosphere.2023.139630).

48 A. Talha Khalil, S. Hameed, S. Afridi, H. E. A. Mohamed and Z. K. Shinwari, *Sageretia thea* mediated biosynthesis of metal oxide nanoparticles for catalytic degradation of crystal violet dye, *Mater. Today: Proc.*, 2021, **36**, 397–400, DOI: [10.1016/J.matpr.2020.04.687](https://doi.org/10.1016/J.matpr.2020.04.687).